

PREDICTIVE POWER CONTROL FOR DYNAMIC STATE ESTIMATION OVER WIRELESS SENSOR NETWORKS WITH RELAYS

Jan Østergaard, Daniel E. Quevedo, and Anders Ahlén

Department of Electronic Systems
Aalborg University
Aalborg, Denmark
janoe@ieee.org

School of Electrical Engineering
& Computer Science
The University of Newcastle
Newcastle, Australia
dquevedo@ieee.org

Department of Engineering Sciences,
Signals and Systems
Uppsala University
Uppsala, Sweden
anders.ahlen@signal.uu.se

ABSTRACT

We present a predictive power controller for state estimation of a stationary ARMA process over a wireless sensor network (WSN), consisting of sensor nodes, relays, and a single gateway (GW). The state estimate is formed centrally at the GW by using packets received from sensors and relays. The latter perform network coding of sensor measurements.

Communication from sensors and relays to the GW is over a fading channel. Packet loss probabilities depend upon the time-varying channel gains and the transmission powers used. To achieve an optimal trade-off between state estimation quality and energy expenditure, in our approach the GW decides upon the in general time-varying transmission powers of sensors and relays. This decision process is carried out on-line and adapts to changing channel conditions by using elements of stochastic model predictive control. Simulations on measured channel data illustrate the performance achieved by the proposed controller.

1. INTRODUCTION

Wireless sensor networks (WSNs) have recently emerged as an important alternative to wired sensor networks for a widespread of applications, e.g., target-tracking and data acquisition [5, 15]. A WSN typically consists of several sensor nodes and perhaps a few control nodes. The sensor nodes are equipped with a sensing component (to measure e.g., temperature), a processing device (to perform simple computations on the measured raw data), and a communication device, e.g., a transceiver (to communicate with the control nodes and perhaps nearby sensor nodes). A relay can be introduced either to increase coverage or to improve performance, be it increase accuracy, throughput or robustness. A relay can also be part of a higher layer in a hierarchical network. As such it can be either more capable or have more available energy.

The wireless communication channel between nodes in the WSN is subject to fading, which frequently causes packet errors. A key aspect is that the time-variability of the fading channel can be alleviated by dynamically adjusting the power levels. Whilst to keep packet error rates low, high transmission power should be used, this is rarely an option in WSNs, since in most applications sensor nodes are expected to be operational for several years without the replacement of batteries; see, e.g., [7, 17]. Another aspect is that many of the available sensor nodes have a constrained transmission power.

In the present work, we consider a WSN architecture having M sensor nodes, J relays and a single GW. The WSN is set up to provide estimates of the state vector sequence $\{x(k)\}$ of a stationary process described via

$$x(k+1) = Ax(k) + w(k), \quad k \in \{0, 1, \dots\}, \quad (1)$$

where the initial state $x(0) \in \mathbb{R}^n$ is zero-mean Gaussian distributed with covariance matrix P_0 and the noise process $\{w(k)\}$ is i.i.d. zero-mean Gaussian distributed with covariance matrix Q .

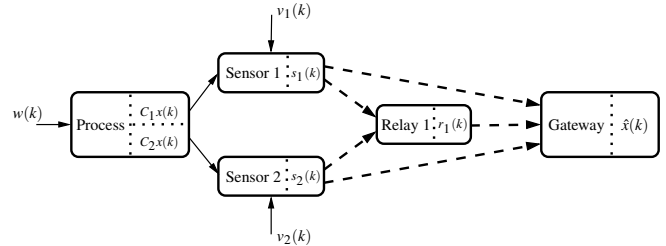


Figure 1: Centralized state estimation with a WSN having $M = 2$ sensors and $J = 1$ relays. The dashed lines denote fading channels which introduce random transmission errors.

Each sensor $m \in \{1, \dots, M\}$, provides noisy measurements given by

$$y_m(k) = C_m x(k) + v_m(k), \quad k \in \{0, 1, \dots\}, \quad (2)$$

where $\{v_m(k)\}$ is i.i.d. zero-mean Gaussian distributed with covariance matrix R_m . The measurements in (2) are quantized (with a given uniform quantizer) and transmitted at an appropriate power level over a fading channel (causing random packet loss) to the gateway and relays. The latter perform network coding and forward processed sensor measurements whenever appropriate to the GW. To avoid interference between nodes, the communication channel is accessed in a TDMA fashion with a pre-designed protocol.

At the GW, received packets from the sensors and relays are then used to estimate $x(k)$ by means of an appropriate time-varying Kalman Filter. Fig. 1 depicts a simple instance of the overall configuration of the system under study.

The main contribution of this paper is to present a centralized predictive controller for sensor and relay transmission power levels within the WSN architecture examined. The controller is located at the GW and trades off energy use for estimation accuracy. The present work complements our recent papers, such as [10, 12, 13], to encompass WSNs with relays. The extension proposed in the present work will be shown to have the potential to give significant performance gains.

2. QUANTIZATION AND NETWORK CODING

Before developing the power controller in Section 5, we will first describe some aspects of the WSN configuration which are relevant to the state estimation problem at hand. For this purpose, in this section, we will focus on quantization and network coding, whereas in Section 3 we will discuss communication issues.

2.1 Quantization

Throughout this work, we will be using standard high-resolution source coding results [4].

Each sensor node is equipped with an encoder which maps the measurement (i.e., the *source symbol*) $y_m(k) \in \mathbb{R}$ to a sequence of

Data successfully received	Values reconstructed
$s_1(k), s_2(k), r_1(k)$	$\hat{y}_1(k), \hat{y}_2(k)$
$s_1(k), s_2(k)$	$\hat{y}_1(k), \hat{y}_2(k)$
$s_1(k), r_1(k)$	$\hat{y}_1(k), \hat{y}_2(k)$
$s_2(k), r_1(k)$	$\hat{y}_1(k), \hat{y}_2(k)$
$s_1(k)$	$\hat{y}_1(k)$,
$s_2(k)$	$\hat{y}_2(k)$
$r_1(k)$	none
none	none

Table 1: Reconstructed values at the GW of the WSN in Fig. 1 with network coding as described in Section 2.2.

bits, say $s_m(k)$, so that the average bitrate is b_m . More specifically, the encoder at sensor m consists of two components: a scalar uniform quantizer \mathcal{Q}_m and an entropy encoder \mathcal{E}_m . The decoder (which is located at the GW) also has two components; an entropy decoder and the reconstruction function which outputs $\hat{y}_m(k)$.

Under high-resolution assumptions, it is known that the rate b_m of an entropy-constrained scalar quantizer is given by¹

$$b_m \approx H(\hat{y}_m(k)) \approx h(y_m(k)) - \log_2(\Delta_m) \quad (3)$$

where $H(\hat{y}(k))$ denotes the discrete entropy of the quantized (discrete) random variable $\hat{y}(k)$, $h(y_m(k))$ denotes the differential entropy of the random variable $y_m(k)$ and Δ_m denotes the stepsize of the uniform scalar quantizer. For simplicity, we will in the sequel assume that $\{y_m(k)\}_{k=0}^{\infty}$ is a stationary process with $y_m(k)$ being zero-mean Gaussian with variance $\sigma_{y_m}^2$. Its differential entropy is then given by $h(y_m(k)) = \frac{1}{2} \log_2(2\pi e \sigma_{y_m}^2)$. Under high-resolution assumptions, it is known that the expected distortion D_m (in the mean squared error sense, i.e. $D_m = \mathbb{E}\|y_m(k) - \hat{y}_m(k)\|^2$) of an entropy-constrained scalar uniform quantizer satisfies

$$D_m \approx \frac{\pi e}{6} \sigma_{y_m}^2 2^{-2b_m} \quad (4)$$

where the rate b_m is given in (3).

The sensor measurements need to be encoded, i.e., converted into a bit-stream, before they can be transmitted to the GW. A simple but efficient coding method is scalar uniform quantization followed by scalar entropy coding. Thus, $y_m(k)$ is quantized using the quantizer \mathcal{Q}_m resulting in the index $i_m(k)$, which refers to a codeword in the quantizer's codebook. This index is further entropy coded and the resulting bit-stream of length b_m bits is denoted $s_m(k)$. At the gateway, the index $i_m(k)$ is recovered by using the appropriate entropy decoder and the reconstruction $\hat{y}_m(k)$ is obtained simply as the $i_m(k)$ -th codeword in the codebook of the chosen quantizer. A scalar uniform quantizer with step-size Δ_m can be efficiently implemented without the need of searching for the nearest element in a codebook by simply scaling $y_m(k)$ by Δ_m followed by rounding, i.e. by forming $\lfloor y_m(k)/\Delta_m \rfloor$ where $\lfloor \cdot \rfloor$ denotes rounding to the nearest integer. At the gateway, the signal is reconstructed by simply applying the inverse scaling, i.e., we have $\hat{y}_m(k) = \lfloor y_m(k)/\Delta_m \rfloor \Delta_m$. In principle, the quantizer has unbounded support but the analog to digital converter in the sensor bounds the support of the input to the quantizer. Furthermore, the quantized output needs to be entropy encoded before being transmitted to the gateway. The entropy coder consists of a codebook, which due to memory considerations cannot be arbitrarily large. In practice, we choose the size of the codebooks so that the probability of falling outside the support of the entropy coder is very small and the impact of the outliers on the total distortion is therefore negligible.

2.2 Network Coding

In traditional networks, intermediate nodes are limited to (or only permitted to) perform simple operations on the incoming data, such

¹The approximation becomes exact in the limit as the distortion tends to zero (or equivalently as the rate diverges to infinity) [4].

as duplication and forwarding. Moreover, traditionally there has been a preference to avoid data ‘‘collisions’’ at intermediate nodes. With network coding, on the other hand, the intermediate network nodes are allowed to mix² the incoming data in such a way that the original data can be recovered at the network edges. This increased flexibility in the network architecture generally provides a more cost-efficient transportation of information [1, 3, 18].

In the present work, the relays act as intermediate network nodes and are able to perform simple network coding on the data. As illustrated in Fig. 1, the relays are overhearing broadcast communication from the sensors to the GW, and are therefore able to aid the GW with additional information about the sensors' data. In particular, the relays will XOR the incoming data at a bit level, i.e., without decoding, see [3].

For example, consider the WSN in Fig. 1 and assume that the GW has received either only $s_1(k)$ or only $s_2(k)$, but the relay has received both $s_1(k)$ and $s_2(k)$. Then, if the relay successfully transmits

$$r_1(k) = s_1(k) \oplus s_2(k) \quad (5)$$

to the GW, then the GW is able to recover both $s_1(k)$ and $s_2(k)$ by use of its own message $s_1(k)$ or $s_2(k)$. The situation is depicted in Table 1.

At the sensors, we may aggregate data in buffers before broadcasting. If the sensor buffers are not of the same size (measured in bits) or, more generally, if the bit-streams received by the relays are not of the same size (in bits), then the relay might have to spend additional bits on informing the GW about the symbol sizes in order to guarantee that the GW can successfully recover the coded data. In this respect, it is worth mentioning that the individual symbols $s_i(k)$ have varying lengths, since we are using variable length quantization. However, the network coding must be applied on symbols of equal length. At the relay, we therefore simply zero pad the shortest symbols in order to make them all of equal length. By using uniquely decodable entropy codes, there will be no confusion at the GW, as of what the length of the individual symbols are. This is so, since no codeword is part of another codeword (in the same code). The average bit-rate at the relay, is therefore upper bounded by

$$b_j^r \leq \sum_{i_1, \dots, i_M} p_{i_1} \cdots p_{i_M} \max\{|s_{i_1}|, \dots, |s_{i_M}|\}, \quad (6)$$

where $|s_{i_m}|$ denotes the cardinality, i.e., the size in bits, of the i_m th symbol (codeword) transmitted by the m th sensor, and p_{i_m} is the corresponding probability of receiving that symbol.

3. COMMUNICATION ASPECTS

Since the communication medium is wireless, several issues arise. These are discussed in the present section.

3.1 Communication Protocol

To avoid the nodes to interfere with each other, in the present work, communication is assumed to be scheduled in a TDMA fashion. The transmission protocol is periodic and pre-defined. Furthermore, all devices are half-duplex, i.e., they cannot transmit and receive at the same time.

For ease of exposition, we will adopt a simple protocol, wherein at the instants $k \in \{0, 1, \dots\}$, all M sensors take measurements $y_m(k)$ and form the symbols $s_m(k)$. These values are then successively broadcast during the TDMA time slots $t \in \{0, 1, \dots, M-1\}$. During time slots $t \in \{M, M+1, \dots, M+J-1\}$, the relays may broadcast the values $r_j(k)$. During the last time-slot, namely $t = M+J$, the GW forms the state estimate $\hat{x}(k)$. During that time slot, the GW also transmits the power levels that the sensors and relays are to use at the next instant, $k+1$. A simple instance of this communication protocol is depicted in Fig. 2.

²Typically, only linear combinations of received information is performed [1, 3].

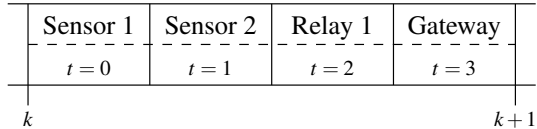


Figure 2: Transmission Protocol with a WSN having $M = 2$ sensors and $J = 1$ relays.

3.2 Transmission Effects

Since communication is over wireless fading channels, random transmission errors will occur. In our approach, corrupted data will be not be used further (save for possible channel gain estimation). We thus model transmission effects by introducing the binary stochastic arrival processes $\gamma_m^{sGW} = \{\gamma_m^{sGW}(k)\}_{k \in \mathbb{N}_0}$, defined via

$$\gamma_m^{sGW}(k) = \begin{cases} 1 & \text{if } s_m(k) \text{ arrives error-free at time } k, \\ 0 & \text{otherwise,} \end{cases} \quad (7)$$

where the superscript sGW denotes the channel between a sensor and the GW. Relay channel effects are modeled in a similar manner, namely, by introducing the binary processes $\gamma_m^{sr}(k)$ and $\gamma_j^{rGW}(k)$ where sr and rGW denote the channel between a sensor and the relay and the channel between the relay and the GW, respectively.

The success probabilities $\lambda_m^\xi(k) \triangleq \mathcal{P}\{\gamma_m^\xi(k) = 1\}$, where $\xi \in \{sGW, sr\}$, satisfy:

$$\lambda_m^\xi(k) = \left(1 - \beta_m^\xi(u_m(k)g_m^\xi(k))\right)^{b_m}. \quad (8)$$

In (8), b_m denotes the packet length (which we take equal to the bit-rate, see (3)), $g_m(k)$ refers to the channel power gain, i.e., the square of the magnitude of the complex channel³, $u_m(k)$ is the transmission power used by the m th sensor radio power amplifier, and $\beta_m(\cdot): [0, \infty) \rightarrow [0, 1]$ is the bit-error rate (BER). The latter is a monotonically decreasing function, which depends on the modulation scheme employed, see, e.g., [11, 12], for specific cases.

Similarly, the success probabilities $\lambda_j^{rGW}(k) \triangleq \mathcal{P}\{\gamma_j^{rGW}(k) = 1\}$, $j \in \{1, 2, \dots, J\}$ are given by

$$\lambda_j^{rGW}(k) = \left(1 - \beta_j^{rGW}(\mu_j(k)g_j^{rGW}(k))\right)^{b_j}, \quad (9)$$

where $\mu_j(k)$ and $b_j^{rGW}(k)$ are the power and bit-rate used by the j th relay, respectively; $g_j^{rGW}(k)$ is the channel gain between the j th relay and the GW, and $\beta_j^{rGW}(\cdot): [0, \infty) \rightarrow [0, 1]$ is the BER of the corresponding relay channel.

3.3 Power Issues

It follows from (8) and (9), that one can improve transmission reliability and, thus, state estimation accuracy for a given wireless propagation environment by simply increasing the power levels used by the transmitters. However, in WSNs it is of fundamental importance to save energy. Thus, transmission powers are a precious resource. In Section 5, we will present a control method, where transmission powers are assigned in an on-line manner, with the aim to optimize estimation accuracy without incurring excessive energy use.

Before proceeding, we note that one can quantify the energy used by each sensor $m \in \{1, \dots, M\}$ at a given (discrete) time instant, k , via $E_m(u_m(k))$, where

$$E_m(u_m(k)) \triangleq \begin{cases} u_m(k) \frac{b_m}{\alpha} + E_P & \text{if } u_m(k) > 0, \\ 0 & \text{if } u_m(k) = 0. \end{cases} \quad (10)$$

³Note that $g_m(k)$ is here defined to include also path-loss, power amplifier efficiency, antenna gain and noise figure.

γ_1^{sGW}	γ_2^{sGW}	γ_1^{sr}	γ_2^{sr}	γ_1^{rGW}	γ_1	γ_2
1	1	1	1	1	1	1
1	1	1	0	0	1	1
1	1	0	1	0	1	1
1	1	0	0	0	1	1
1	0	1	1	1	1	1
0	1	1	1	1	1	1
1	0	1	0	0	1	0
1	0	0	1	0	1	0
1	0	0	0	0	1	0
0	1	1	0	0	0	1
0	1	0	1	0	0	1
0	1	0	0	0	0	1
0	0	1	1	1	0	0
0	0	1	0	0	0	0
0	0	0	1	0	0	0
0	0	0	0	0	0	0

Table 2: Reconstruction processes of the WSN in Fig. 1 with network coding as described in Section 2.2. Note that the relay transmits only if it has received both s_1 and s_2 .

In (10), E_P denotes the processing cost, i.e., the energy needed for wake-up, circuitry and sensing and α is the channel bit-rate.

Due to physical limitations of the radio power amplifiers, the transmission power levels of the sensors are constrained, for given values $\{u_m^{\max}\}$, according to:

$$0 \leq u_m(k) \leq u_m^{\max}, \quad \forall k \in \mathbb{N}_0, \quad \forall m \in \{1, 2, \dots, M\}. \quad (11)$$

The energy consumption of the relays can be quantified similarly by introducing energy functions $E_j^r(\mu_j(k))$ and constraints $\{\mu_j^{\max}\}$. Note that the relays transmit only if the sensor data needed to perform network coding has been successfully received, see Section 2.2.

4. FORMING THE STATE ESTIMATE

To formulate the state estimate, it is useful to introduce the reconstruction processes, $\gamma_m(k)$, defined via:

$$\gamma_m(k) = \begin{cases} 1 & \text{if } \hat{y}_m(k) \text{ can be reconstructed at time } k, \\ 0 & \text{otherwise} \end{cases} \quad (12)$$

Since the relays employ network coding, the values $\gamma_m(k)$ are a deterministic function of the processes $\gamma_m^{sGW}(k)$, $\gamma_m^{sr}(k)$ and $\gamma_j^{rGW}(k)$ introduced in Section 3.2. For example, for the case given in Table 1, the processes $\gamma_1(k)$ and $\gamma_2(k)$ are determined as per Table 2.

We will assume that the gateway knows, whether packets received from the sensors and relays contain errors or not. Thus, at any time k , past and present realizations of the overall reconstruction process, i.e., $\{\gamma_m(k-\ell)\}_{\ell \geq 0, m \in \{1, \dots, M\}}$, are available at the gateway. A key aspect here is that, for state estimation purposes, the system amounts to sampling (1)-(2) only at the successful transmission instants of each sensor link. Consequently, the time-varying Kalman filter for the system (1) with output matrix

$$C(k) \triangleq [\gamma_1(k)C_1 \quad \dots \quad \gamma_M(k)C_M]^T \quad (13)$$

gives the best linear state estimates; see, e.g., [16]. These are given by: $\hat{x}(k+1) = A\hat{x}(k) + K(k+1)(\hat{y}(k+1) - C(k+1)A\hat{x}(k))$, where

$$\begin{aligned} \hat{y}(k+1) &\triangleq [\hat{y}_1(k) \quad \hat{y}_2(k) \quad \dots \quad \hat{y}_M(k)]^T \\ K(k) &\triangleq P(k)C(k)^T (C(k)P(k)C(k)^T + R(k))^{-1} \\ P(k+1) &\triangleq AP(k)A^T + Q - AK(k)C(k)P(k)A^T \\ R(k) &\triangleq \text{diag}(R_1 + D_1, \dots, R_M + D_M), \end{aligned} \quad (14)$$

with $\{D_m\}$ being the distortions due to quantization, see (4). The recursion in (14) is initialized with $P(0) = P_0$, $\hat{x}(0) = 0$.

5. ON-LINE DESIGN OF POWER LEVELS

We have seen that designing the sensor and relay transmission powers involves a trade-off between transmission error probabilities (and, thus, state estimation accuracy) and energy use. We will next present a controller which optimizes this trade-off over a future prediction horizon. The controller is located at the gateway (control node). Its output contains information on the power levels to be used by the M sensors and J relays.

5.1 Signaling

To save signal processing energy at the sensors and relays, we would like to limit power control signaling as much as possible. In particular, the command signal for each sensor and relay will contain finitely quantized power increments, say $\delta u_m(k)$ and $\delta \mu_j(k)$ rather than the actual power values, $u_m(k)$ and $\mu_j(k)$. Upon reception of these increments the power level to be used by the radio power amplifiers are selected by simply setting

$$\begin{aligned} u_m(k) &= u_m(k-1) + \delta u_m(k), & m \in \{1, \dots, M\} \\ \mu_j(k) &= \mu_j(k-1) + \delta \mu_j(k), & j \in \{1, \dots, J\}. \end{aligned}$$

5.2 Predictive Control

In order to trade energy consumption for estimation cost, at each time instant k , the proposed controller examines the finite horizon cost function

$$V(k) = V_1(k) + \rho V_2(k), \quad (15)$$

where $\rho \geq 0$ is a design parameter and

$$V_2(k) \triangleq \sum_{\ell=k+1}^{k+N} \left(\sum_{m=1}^M E_m(u_m(\ell)) + \sum_{j=1}^J E_j^r(\mu_m(\ell)) \right) \quad (16)$$

is the predicted energy consumption of the sensors and relays over a horizon N . In (15),

$$V_1(k) \triangleq \sum_{\ell=k+1}^{k+N} \mathbb{E} \{ \text{trace} \{ \bar{P}(\ell) \} \} \quad (17)$$

quantifies the estimation cost through the expected trace of⁴

$$\bar{P}(k) = P(k) - K(k)C(k)P(k). \quad (18)$$

Expectation in (17) is with respect to $\{\gamma_m(k)\}$, i.e., the set of possible reconstruction outcomes, see (12). The probability mass distribution of this set depends through the different transmission outcomes upon the decision variables, i.e., the power level increments.

At every time instant k (and during its assigned time slot), the predictive controller finds the optimal values $\{\delta u_m(k)\}$ and $\{\delta \mu_j(k)\}$ through a brute-force search strategy, where the cost function $V(k)$ is evaluated for all possible combinations of power level increments over the prediction horizon. As noted in Section 5.1, power level increments are quantized, putting the optimization problem into the context of those arising in quantized predictive control, see also [14].

Following the moving horizon principle, (see, e.g., [6, 8, 9]), at the next time instant, namely $k+1$, a new optimization is carried out with fresh data and a shifted prediction horizon. This gives rise to power control increments $\{\delta u_m(k+1)\}$ and $\{\delta \mu_j(k+1)\}$. The procedure is repeated on-line and *ad-infinitum*.

The prediction horizon N allows the designer to trade-off performance versus on-line computational effort, larger horizons giving, in general, better performance since more information is taken into account in the decision process, cf. [6].

It is worth emphasizing that minimization of $V(k)$ in (15) requires channel gain predictions over the prediction horizon $\{k+$

$1, k+2, \dots, k+N\}$. Whilst obtaining such predictions at the GW side for the channels involving the GW is simple⁵, predicting the channel gains from the sensors to the relays at the GW side is difficult. Fortunately, as will become apparent in Section 6 below, the proposed control algorithm gives good performance, even if the channel gains from the sensors to the relays are not predicted accurately.

6. SIMULATIONS

To illustrate the performance of the proposed power control method, we next present simulations, which use real channel measurements.

6.1 System Setup

We consider a system model (1) with $A = \begin{bmatrix} 1.6718 & -0.9948 \\ 1 & 0 \end{bmatrix}$, $Q = 1/2I$, and $P_0 = 0.3I$.

We simulate a WSN having $M = 2$ sensors with $C_1[1 \ 0]$, $C_2 = [0 \ 1]$, and variances $R_1 = R_2 = 1/100$. We use one relay, which can be either on or off, a decision which is taken by the GW. When the relay is on, it uses a constant power level of $\mu(k) = 6 \times 10^{-5}$. Moreover, if the relay successfully receives $s_1(k)$ and $s_2(k)$ at some time k , then it performs network coding, by simply XOR-ing the two bit sequences. If only a single signal value is received by the relay, it remains quiet. In the simulations, we have fixed the average bit-rate of the sensors to $b_m = 8$ bit/dim. With this, we construct Huffman entropy codes for the two sensors. Using these entropy codes in (6), we find that the average maximum symbols length, which is equal to the average rate of the relay, is upper bounded by 8.57 bit/dim. Thus, the rate of the relay is only slightly larger than that of the sensors. The power of the sensors is restricted to the interval $0 \leq u_m(k) \leq 3 \times 10^{-4}$ and the power increments are restricted to $\pm 3 \times 10^{-5}$. We use a prediction horizon of $N = 1$. This only requires one step predictions of the channel gains.

6.2 Scheduling

We use the scheduling policy depicted in Fig. 2, where each node is taking turns with a period of $T = M + J + 1 = 4$ cycles. At time slot $t = 0$, the first sensor broadcasts $s_1(0)$. At time slot $t = 1$, the second sensor broadcasts $s_2(0)$. During these broadcasts, the relay and the GW have been listening. At time slot $t = 2$, if the relay has successfully received both $s_1(0)$ and $s_2(0)$, then it forms $r(0) = s_1(0) \oplus s_2(0)$ and transmits this network coded symbol to the GW, see (5). If the relay has not successfully received both symbols $s_1(0)$ and $s_2(0)$, then, in order to save power, it does not transmit anything.

At this point, the gateway forms the best estimate of $x(0)$ using the Kalman filter described in Section 4 and which takes into account all received information. The GW then uses the power control algorithm proposed in Section 5 to calculate optimal values for the next period, i.e., optimal power increments for the sensors and decides whether or not to turn on the relay. Thus, in a single time slot, i.e., at $t = 3$, the GW broadcasts to both sensor nodes as well as to the relay. At time instant $k = 1$, the procedure is repeated, starting at the first sensor, which transmits $s_1(1)$ and so on.

6.3 Results

In the simulations we have normalized the energy by varying ρ so that the sensors and the relay use the same amount of energy in all cases, see Table 3. Thus, the predictive controller seeks to distribute the available energy between the sensor nodes and the relay to minimize the state estimation error variance.

Our baseline scenario is without relay and network coding, but where the sensor power levels are controlled [12]. If an uncontrolled

⁴If the quantization noise was Gaussian and i.i.d., then $\bar{P}(\ell)$ would correspond to the conditional posterior covariance of $\hat{x}(k)$; see, e.g., [12, 16].

⁵Channel predictions can be obtained by using techniques described, e.g., in [2].

ρ	V_1	$V_2 [nJ]$	Relay Channel Models	Gain V_1	System
10^6	0.0707	63.21	–	–	Baseline (no relay)
10^8	0.2021	63.77	Sensor-Relay (predicted), Relay-GW (predicted)	–	Relay always on
655000	0.0341	63.11	Sensor-Relay (known), Relay-GW (known)	51.77%	Relay on/off
680000	0.0382	63.11	Sensor-Relay (predicted), Relay-GW (predicted)	45.87%	Relay on/off
430000	0.0682	63.12	Sensor-Relay (fixed at -100 dB), Relay-GW (predicted)	3.54%	Relay on/off
560000	0.0391	63.11	Sensor-Relay (fixed at -105 dB), Relay-GW (predicted)	44.70%	Relay on/off
1003000	0.0375	63.11	Sensor-Relay (fixed at -110 dB), Relay-GW (predicted)	46.96%	Relay on/off
2080000	0.0429	63.11	Sensor-Relay (fixed at -115 dB), Relay-GW (predicted)	39.32%	Relay on/off

Table 3: Performance.

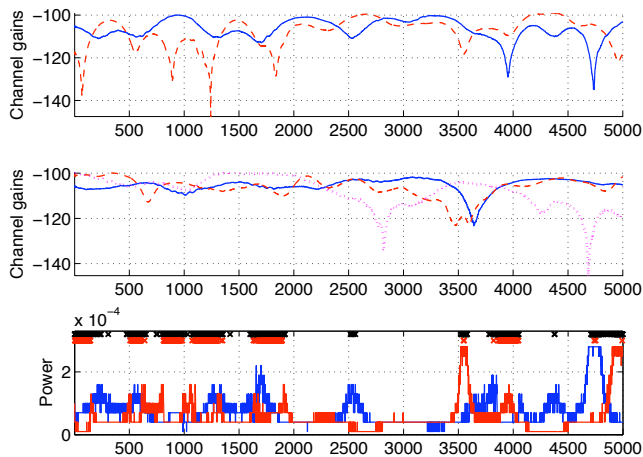


Figure 3: Relay and sensors are controlled by GW by using the controller proposed in Section 5. In this case we assume perfect channel predictions of all channels. The relay is successful in 764 out of 1291 instances, i.e., 59.18% efficiency.

relay which is *on* all the time is used, then the relay uses most of the available energy leaving very little to the sensors to spend. As a consequence the performance, as measured by V_1 , will be significantly worse than the base line scenario, cf. Table 3. Even though the network coding helps, the always-on strategy wastes energy on the relay when it is not needed. Significantly better performance can be obtained if the power controller also manages the relay, as proposed in Section 5. In fact, if we let the controller decide whether the relay shall be on or off, and if we use known or predicted channel gains on all channels, then, according to Table 3 we obtain a noteworthy performance increase in V_1 of almost 52% (known channels) and 46% (predicted channels), respectively. In Fig. 3 the top diagram illustrates the channel gains between the sensors and the GW and the bottom diagram illustrates the chosen power levels of the two sensors. The blue curves correspond to sensor 1, and the red curves to sensor 2. The black crosses indicate the time slots where the GW has decided to turn on the relay. The red crosses, on the other hand, indicate when the relay operation was successful, i.e., when the relay received $s_1(k)$ and $s_2(k)$ without errors and furthermore successfully transmitted $r(k) = s_1(k) \oplus s_2(k)$ to the GW. The exact numbers of black and red crosses are provided in the figure text. The middle diagram show the channel gain from the sensors to the relay (sensor 1: blue solid line, sensor 2: red dashed line) as well as the channel gain from the relay to the GW (dotted line).

It is clear from Fig. 3, that the controller trades off energy spent on the sensors for energy spent on the relay. Only at the deepest drops in the sensor-GW channel gains beyond time 3500 are the control actions saturated at the sensors. We note that it is beneficial to rely on the relay and network coding most of the time.

We have also simulated the situation where the relay uses a fixed average channel estimate for the sensor-relay channels. In this case, we conclude that it is safer to underestimate the sensor-relay

channel gains than to overestimate them, see Table 3.

REFERENCES

- [1] R. Ahlswede, N. Cai, S.-Y. R. Li, and R. W. Yeung. Network information flow. *IEEE Trans. Inform. Theory*, 46:1204–1216, 2000.
- [2] T. Ekman, M. Sternad, and A. Ahlén. Unbiased power prediction of Rayleigh fading channels. In *Proc. Vehicular Technology Conf.*, volume 1, pages 280–284, 2002.
- [3] C. Fragouli, J.-Y. Le Boudec, and J. Widmer. Network coding: an instant primer. *SIGCOMM Comput. Commun. Rev.*, 36(1):63–68, Jan. 2006.
- [4] A. Gersho and R. M. Gray. *Vector Quantization and Signal Compression*. Kluwer Academic, Boston, MA, 1992.
- [5] H. Gharavi and S. P. Kumar. Special section on sensor networks and applications. *Proc. IEEE*, 91(8):1151–1152, Aug. 2003.
- [6] G. C. Goodwin, M. M. Serón, and J. A. De Doná. *Constrained Control & Estimation – An Optimization Perspective*. Springer Verlag, London, 2005.
- [7] M. Johansson, E. Björnemo, and A. Ahlén. Fixed link margins outperform power control in energy-limited wireless sensor networks. In *Proc. IEEE Int. Conf. Acoust. Speech Signal Process.*, volume 3, pages 513–516, Honolulu, HI, 2007.
- [8] J. M. Maciejowski. *Predictive Control with Constraints*. Prentice-Hall, Englewood Cliffs, N. J., 2002.
- [9] D. Q. Mayne, J. B. Rawlings, C. V. Rao, and P. O. M. Scokaert. Constrained model predictive control: Optimality and stability. *Automatica*, 36(6):789–814, June 2000.
- [10] J. Østergaard, D. E. Quevedo, and A. Ahlén. Predictive power control and multiple-description coding for wireless sensor networks. In *Proc. IEEE Int. Conf. Acoust. Speech Signal Process.*, Taipei, Taiwan, 2009.
- [11] J. G. Proakis. *Digital Communications*. McGraw-Hill, New York, N.Y., 3rd edition, 1995.
- [12] D. E. Quevedo and A. Ahlén. A predictive power control scheme for energy efficient state estimation via wireless sensor networks. In *Proc. IEEE Conf. Decis. Contr.*, Cancún, México, Dec. 2008.
- [13] D. E. Quevedo, A. Ahlén, and J. Østergaard. Energy efficient state estimation with wireless sensors through the use of predictive power control and coding. *IEEE Trans. Signal Processing*, 2010. Accepted for publication.
- [14] D. E. Quevedo, G. C. Goodwin, and J. A. De Doná. Finite constraint set receding horizon quadratic control. *Int. J. Robust Nonlin. Contr.*, 14(4):355–377, Mar. 2004.
- [15] X. Shen, Q. Zhang, and R. Caiming Qiu. Wireless sensor networking. *IEEE Wireless Commun.*, 14(6):4–5, Dec. 2007.
- [16] T. Söderström. *Discrete-Time Stochastic Systems*. Prentice Hall, 1994.
- [17] J.-J. Xiao, S. Cui, Z.-Q. Luo, and A. J. Goldsmith. Linear coherent decentralized estimation. *IEEE Trans. Signal Processing*, 56(2):757–770, Feb. 2008.
- [18] R. W. Yeung, S.-Y. R. Li, N. Cai, and Z. Zhang. *Network Coding Theory*. now Publishers, 2005.